

Genesis of Vesicle-Like and Tubular Morphologies in Inorganic Precipitates: Amorphous Mo Oxyulfides

Pavel Afanasiev* and Igor Bezverkhly

Institut de Recherches sur la Catalyse, 2, Avenue Albert Einstein, 69626 Villeurbanne Cedex, France

Received: July 18, 2002; In Final Form: October 28, 2002

Amorphous molybdenum oxosulfide precipitation in the acetone–water mixed solvent leads to the variety of original morphologies, including entangled tubules, hollow spheres, and sponge-like fractal structures. The dominating type of morphology obtained can be controlled by the variations of the amount of different electrolytes present in the reaction mixture, such as NH_4SCN , KCl , $(\text{NH}_4)_2\text{SO}_4$, or $(\text{NH}_2\text{OH})_2\text{HSO}_4$. The qualitative analogy between the observed behavior and vesiculation of lipids is discussed.

Introduction

Since the discovery of carbon nanotubes,¹ the intense research in this field provided many examples of different solids possessing tubular morphology, both at the nanometer and micrometer size scales. In most cases the tubules are produced due to well-understood physical mechanisms, such as the strain release in the incommensurate lamellar structures² or self-organization of the organic surfactant templates.³ However, several recent syntheses of inorganic tubules do not fit into any of the known categories. Among them are, for example, the amorphous phosphorus nitride⁴ and molybdenum sulfide hollow tubes,^{5,6} for which physical mechanism of the tubules and hollow spheres formation is unclear. However, despite very different chemistry involved, the reported syntheses have some important similarity: the inorganic solids obtained are amorphous, whereas hollow or filled spheres and tubules coexist in them. As for the preparation conditions, they are carried out in the mixed solvents in the presence of dissolved electrolytes. The important point is that no external surfactant was added to the reaction mixtures to obtain such structures.

These observations made us suggest that a general self-organization mechanism exists, leading to the amorphous hollow balls and tubules. This mechanism is supposed to be somewhat similar to that known for the micelles formation and vesiculation of lipids. Here we illustrate the qualitative consequences following from this hypothesis, showing that the morphology of the amorphous molybdenum polysulfide might be controlled by the change of the ionic strength of the reaction mixture. Moreover, the types of morphologies similar to those known for the vesicles and tubular membranes are subsequently produced when the synthesis conditions are modified.

In this paper the relationship between the preparation conditions and the morphology of the precipitates was studied for the reaction of $(\text{NH}_4)_2\text{Mo}_2\text{S}_{12}$ (ammonium thiodimolybdate, ATDM) in water–acetone solutions in the presence of varying amounts of different electrolytes, such as NH_4SCN , KCl , $(\text{NH}_4)_2\text{SO}_4$, or $(\text{NH}_2\text{OH})_2\text{HSO}_4$.

Experimental Section

In a typical experiment, 3 g of ATDM was refluxed with 200 mL of acetone for 12 h in a Soxhlet apparatus. The resulting washing solution is a stable dark colloidal suspension. After

centrifugation, the brown powder of MoS_{5+x} precipitate was eliminated, and the transparent red-brown solution was collected. For characterization purposes, a part of this solution was evaporated in argon flow and the resulting brown solid **I** was used for analytical purposes. Otherwise, to obtain the solids with organized morphology, the same solution was diluted with aqueous electrolyte solutions. Unless otherwise stated, in all experiments the ratio of water to acetone solutions was 1:10. For example, 20 mL of 5% KCl aqueous solution was added to 200 mL of acetone solution of **I**. The reaction mixture was kept overnight; then the suspension formed was separated by centrifugation, dried, and conserved in argon. The solids morphology was studied on a HITACHI S800 SEM microscope (CMEABG, Université Claude Bernard—Lyon 1). Chemical composition was determined by elemental analysis. The IR spectra were measured in KBr disks on a BRUKER device. The XPS studies were performed on a VG ESCALAB 200R spectrometer using $\text{Al K}\alpha$ radiation. The XPS spectra of S, O, N, and Mo were recorded and their binding energies (BE) referred to the energy of the C 1s peak (BE 284.5 eV). Quantification of the surface contents of the elements was done using the sensitivity factors provided with the VG software. The EXAFS measurements were performed at the Laboratoire d'Utilisation du Rayonnement Electromagnétique (LURE), on the XAS2 spectrometer (line D21). The measurements were carried out in the transmission mode at the Mo K edge from 19900 eV to 21000 eV at 8 K. The EXAFS data were treated with SEDEM⁷ and FEFF⁸ programs.

Results and Discussion

Recently, we used soft chemistry methods to prepare pure or doped molybdenum sulfides in aqueous or organic solutions.^{9,10} It has been shown that the amorphous molybdenum polysulfide issued from the hydrothermal synthesis formed hollow microtubules.⁶ Trying to rationalize and to simplify this preparation we found that the formation of amorphous tubules is not related to any individual compound but might be observed for a wide range of conditions and for different compositions of precipitate. However, it seems obvious that the key intermediate leading to hollow tubes and balls in these preparations is the $\text{Mo}_2\text{S}_{12}^{2-}$ species. Another condition of obtaining tubules was that the sulfide material is synthesized in aerobic conditions.

In the previous study¹¹ we have found that the ultimate products of acid–base or redox condensation of $\text{Mo}_2\text{S}_{12}^{2-}$,

* Corresponding author.

respectively, with HCl and iodine are the stoichiometric amorphous sulfides MoS_5 and MoS_6 . Nonstoichiometric binary sulfides of intermediate composition MoS_{5+x} are formed due to the superposition of acid–base and redox processes when the acetone solution of $(\text{NH}_4)_2\text{Mo}_2\text{S}_{12}$ is refluxed in air. Characterizations by XRD, IR spectroscopy, and EXAFS suggest that all such sulfides have structures similar to that of MoS_3 but contain more abundant S–S bonds. At the same time, in the course of the reflux in air the side products are obtained, soluble in polar organic solvents such as acetone or ethanol, but rapidly precipitated if a large amount of water is added. The last precipitates are rather unstable in air and tend to polymerize with formation of the insoluble amorphous solids. However, the freshly obtained non-dried precipitates can be completely redissolved in acetone. Chemical analysis shows that the solids precipitated with different electrolytes have similar compositions. This is true for all electrolytes tried, including the hydroxylamine salt (the last might have some reducing properties, but as we showed earlier,¹⁰ no reduction of thiomolybdates with hydroxylamine occurs, even upon reflux). Therefore, the mechanism of precipitation upon adding water and electrolytes seems to be that of the salting out.

As might be inferred from the structure of the initial ATDM and from the results of characterizations of the precipitates, the acetone-soluble species, which are salted out by water and electrolyte solutions, contain some derivatives formed from the $\text{Mo}_2\text{S}_{12}^{2-}$ units, probably condensed and/or oxidized with air. Indeed, chemical analysis of the solid **I** obtained by free evaporation of solvent from the reflux solution shows the non stoichiometric composition of general formula $(\text{NH}_4)_{0.8}\text{MoS}_{4.5}\text{O}_{1.4} \cdot 1.5\text{H}_2\text{O}$. Note that the variations of time of ATDM solution reflux may lead to considerable variations of the precipitate composition. For example, reflux for several days leads to the increase of the oxygen content in the solid and at the same time appearance of elementary sulfur in the XRD patterns of precipitates.

Prior to the description of morphology, we present characterizations of the solid **I** which is the generic substance for the production of tubular and vesicle-like derivatives. If not otherwise stated, the properties of the precipitates obtained by salting out are similar to those described for the solid **I**. The XRD patterns of **I** or its precipitation products with electrolytes correspond to virtually amorphous solids, with a very broad maximum in the range of d between 9 and 10 Å. Note that the distance 9–10 Å is very different from that observed earlier in MoS_3 and MoS_{5+x} sulfides.¹¹ In the IR spectra (Figure 1) the product **I** show the Mo–S (474 cm^{-1}) and S–S bonds (536 cm^{-1}), as well as the appearance of the strong band of Mo=O stretching vibrations at 945 cm^{-1} typical for the oxosulfides.^{12,13} The last band suggests that some substitution of Mo–S bonds with oxygen occurs. Vibrations were also observed, attributable to sulfate ($1310, 1180, 1050$, and 670 cm^{-1}). Note that the intensity of bands does not correspond to the relative amounts of the moieties since the strongly polar Mo=O and S=O stretchings have much higher extinction coefficients than the weakly polar Mo–S and S–S bonds.

In the XPS spectra of the solid **I**, a complex signal of molybdenum is seen, consisting of Mo(V) and a small amount of Mo(VI) species. Sulfur S 2p signal reveals the presence of a considerable amount of sulfate (near 10% of total sulfur), probably formed because of oxidation by ambient air. However the most important part of sulfur has a binding energy of 162.4–163.0 eV, that of the S_2^{2-} species corresponding to the S–S bonds. Nitrogen N 1s signal at BE 401.1 eV corresponds to the

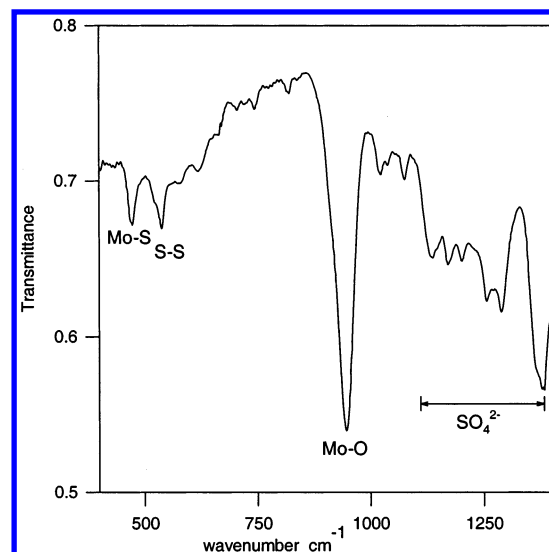


Figure 1. IR spectrum of the amorphous precipitate **I**.

TABLE 1: The XPS Data on the Species Present in the Solid **I**, the Microtubular Solid Obtained from the Solid **I** with 10 % $(\text{NH}_4)_2\text{SO}_4$ and the Amorphous $\text{MoS}_{5.6}$ Sulfide Obtained in the Same Reaction Mixture

sample	Mo 3d		S 2p		O 1s		N 1s	
	BE ^a	R.A. ^a	BE	R.A.	BE	R.A.	BE	R.A.
Solid I	229.3	11	162.4	22	531.8	27	401.2	8
	232.7	0.7	162.9	10				
I + $(\text{NH}_4)_2\text{SO}_4$ (tubules)			168.7	3				
	229.5	8	163.0	29	531.8	30	401.8	7
$\text{MoS}_{5.6}$	232.9	0.5	168.8	4				
	229.3	9	163.0	26	531.8	14	—	—
	232.7	0.8	168.5	3				

^a Binding energy, eV. ^b Relative abundance, % at (surface carbon is not included in the calculation).

ammonium ions. In Table 1 the quantitative analysis is given of the species present in two of the samples under study (solid **I** and its tubular derivative with chemical composition of $(\text{NH}_4)_{0.77}\text{MoS}_{4.46}\text{O}_{1.4} \cdot 2\text{H}_2\text{O}$) and the $\text{MoS}_{5.6}$ binary sulfide as a reference, prepared in similar conditions. It follows from the deconvolution of the XPS peaks of molybdenum that we deal rather with some unique oxosulfide entities than the mixtures of Mo(V) or Mo(IV) sulfide and Mo(VI) oxidized species. Indeed, the amount of individual Mo(VI) species is low; moreover, such species are always present in any dispersed molybdenum sulfide exposed to air.¹⁴ Comparison of spectra with that of a binary sulfide prepared under similar conditions shows that both Mo(VI) and sulfate impurities are present in the samples in comparable amounts. By contrast, the amount of oxygen is significantly higher in the solid **I** and its tubular derivative, suggesting that they contain some bonded oxygen species, which are not present in $\text{MoS}_{5.6}$.

The ensemble of XPS and IR characterizations confirms that the acetone-soluble amorphous product (solid **I**) contains some partially oxidized oligomers of thiomolybdate. Heating of these nonstoichiometric solids in argon or in nitrogen to 773 K leads to the formation of pure MoS_2 compound, which gives indirect proof that molybdenum is bound in them mostly to sulfide or disulfide species.

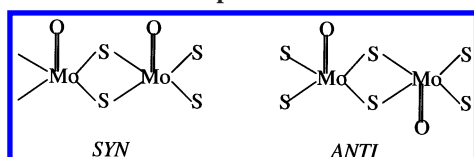
The EXAFS study gives direct insight on the coordination of molybdenum in the precipitates. It showed the presence of at least four neatly distinguishable shells around the central molybdenum atom. The first shell corresponds to a low distance

TABLE 2: Results of Mo Shell EXAFS Fitting in the Amorphous Precipitates Obtained in This Work and MoS_{5.6} Microspheres Produced in a Similar Reaction Mixture (ref 9)

precipitate, (electrolyte added)	<i>R</i> (S) ^a	<i>N</i> (S) ^b	<i>A</i> /Å ^{2c}	<i>R</i> (O)	<i>N</i> (O)	<i>A</i> /Å ²	<i>R</i> (Mo)	<i>N</i> (Mo)	<i>A</i> /Å ^{2c}
(NH ₄) _{0.8} MoS _{4.6} O _{1.5}	2.47	3.8	0.003	1.76	0.7	0.001	2.78	0.9	0.004
(NH ₄) _{0.8} MoS _{4.6} O _{1.5} + 5% (NH ₂ OH ₂)HSO ₄	2.46	4.2	0.003	1.74	0.8	0.001	3.29	1.2	0.003
(tubules)							2.79	0.75	0.003
MoS _{5.6} (ref 11)	2.44	6.2	0.005	-	-	-	3.32	1.2	0.004
							2.76	0.75	0.002

^a Interatomic distance. ^b Coordination number. ^c Debye Waller parameter.

SCHEME 1: Possible Configurations in the Molybdenum Oxosulfide Species



shoulder on the Fourier transform curve. According to the fit, it contains one oxygen atom at the distance 1.76 Å. The second shell contains four sulfur atoms at 2.47 Å. The third and the fourth shells contain Mo atoms at different distances. One Mo neighbor has an *R* value closer to that of bonded Mo—Mo in the amorphous sulfides, whereas the second is obviously a non bonded Mo—Mo interblock distance similar to that reported in the Mo oxosulfides, for example in Mo₂O₂S₉²⁻ salts.¹⁵ As a result of EXAFS characterizations, the precise chemical structure of the species in the precipitates is still not determined and probably it cannot be, since we obviously deal with the complex mixtures of products. However the essential features are reliably established: the species under study are the oligomers which contain the Mo—S—Mo and Mo—S—S—Mo bonds and Mo=O double bonds. Similar moieties are well-known in molybdenum chemistry and correspond to the oligomeric derivatives of MoS₂O₂⁴⁺ core (Scheme 1), which in the considered case are probably coordinated by the S₂²⁻ anions.

The solid **I** by itself has no interesting morphology, being presented by microspheres and shapeless particles of several microns size. It appears, however, that it may generate a variety of original morphologies, provided that several necessary conditions are fulfilled. First of all, the presence of the appropriate amount of water dissolved in acetone is necessary to obtain any anisotropic morphologies. If the reaction was carried out in dry acetone, only the solid **I** and microspherical MoS_{5+x} precipitates were formed, described in ref 11. However, too high amount of water (above 30% vol) leads to the instant formation of shapeless precipitates.

To obtain vesicle-like and tubular structures, the content of the dissolved electrolyte must lie in the appropriate range, depending on its exact chemical composition. Moreover, the electrolyte amount is found to be the key parameter, controlling the morphology obtained.

At low electrolyte content, microspheres are still dominating. However, already at 1% concentration of the electrolyte added, the precipitate morphology is strongly changed. The surface of precipitate is no longer smooth but covered with holes of different size (Figure 4). Larger size holes have notably thickened borders, indicating that after hole formation further redistribution of matter and growth around the hole borders occurs. At the same time, at low electrolyte content large vesicle-like hollow spherical objects are sometimes observed (Figure 5). These objects have walls thickness of several tens of nanometers and their diameter is in the range from one-half to

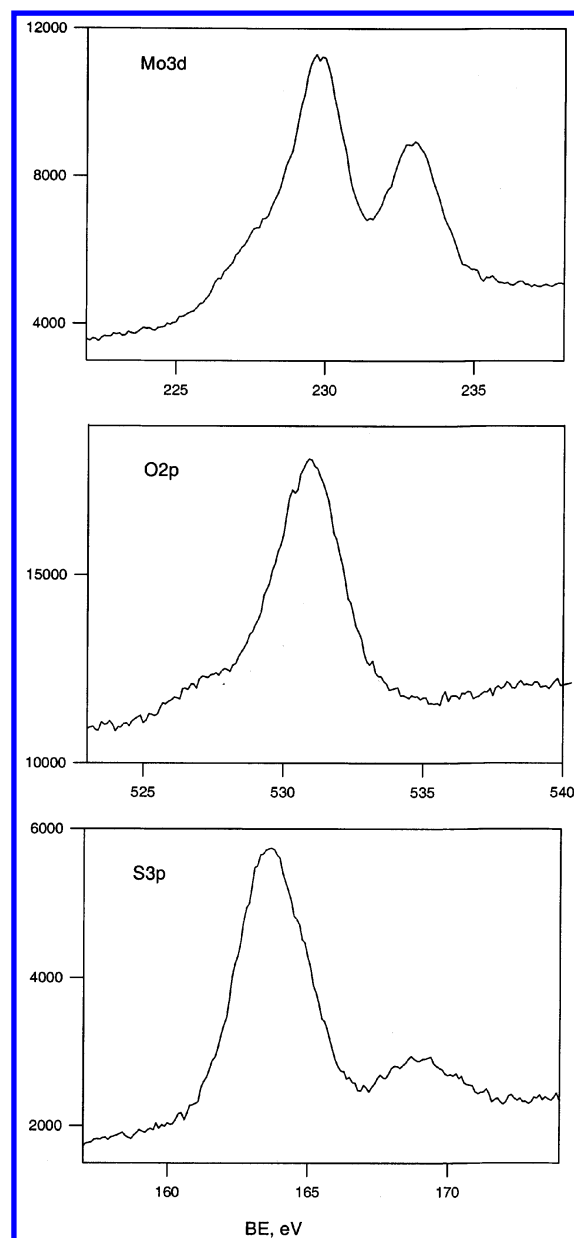


Figure 2. Mo 3d, O 1s, and S 2p XPS spectra of the solid **I**.

several micrometers. Open fragments and cup-like structures observed in the precipitates with low electrolyte content indicate the softness of layers. The broad size distribution of the objects suggests that the free energy of these metastable structures corresponds to flat and ill-defined minima in the variables space (composition—temperature—ionic force). Inhomogeneity of size and variable abundance of the structures also suggest that the difference in the formation energy of such objects is comparable to *kT*.

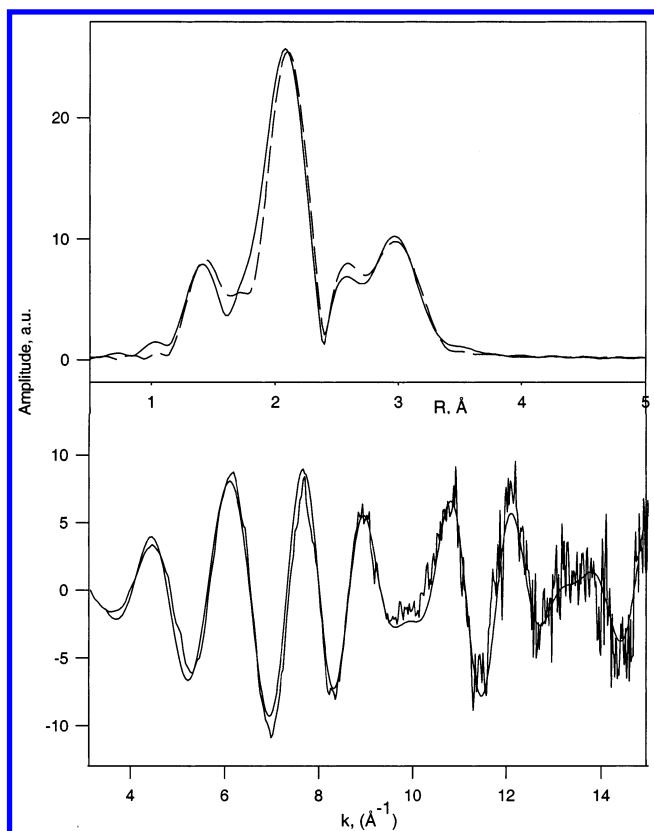


Figure 3. Mo K-edge EXAFS data for the solid **I**, measured at 8 K: the Fourier transform curves of experimental spectrum corrected for the Mo-S first shell backscattering (solid line) and calculated (dashed line).

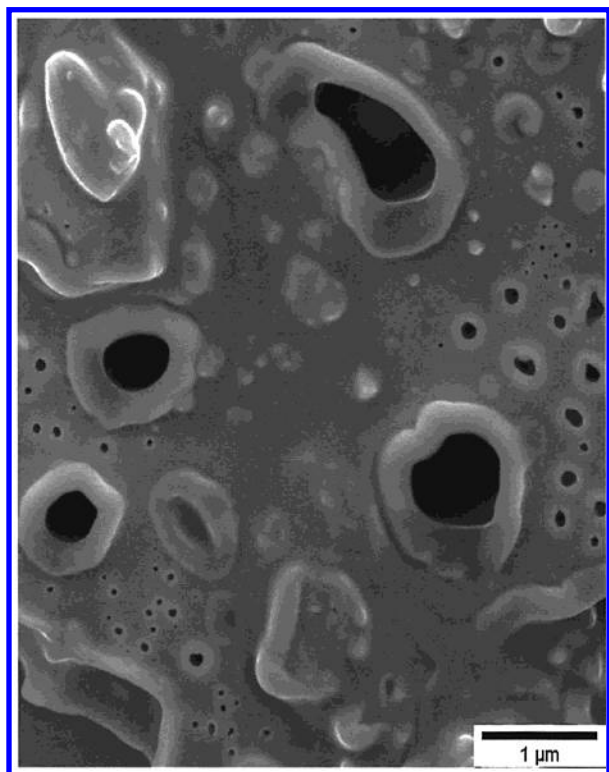


Figure 4. Holey surface of the solid obtained from the solid **I** with 1% $(\text{NH}_4)_2\text{SO}_4$ solution.

Further increase of the electrolyte concentration leads to production of tubular particles similar to those reported earlier.⁵ The tubules are bent and heterogeneous in size, their diameter

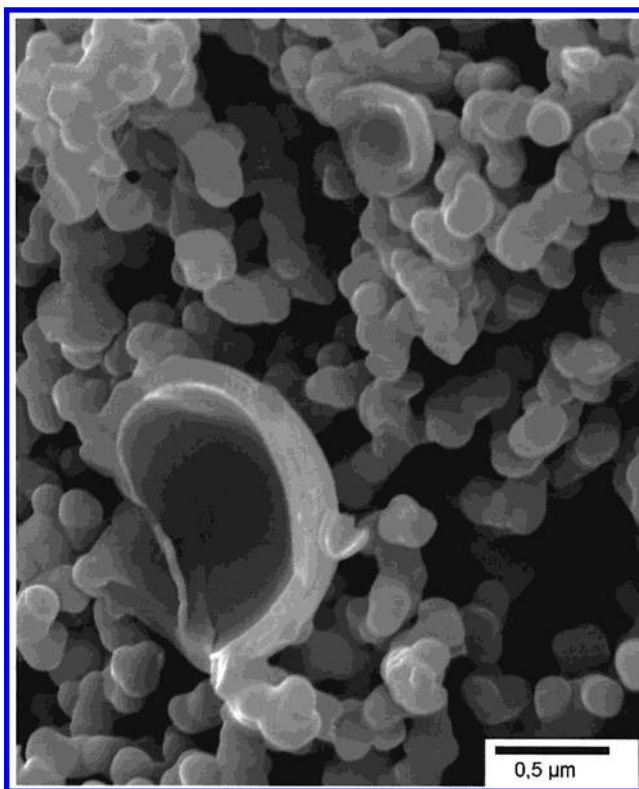


Figure 5. SEM of the precipitates obtained in the presence of 1% $(\text{NH}_2\text{OH})\text{H}_2\text{SO}_4$.

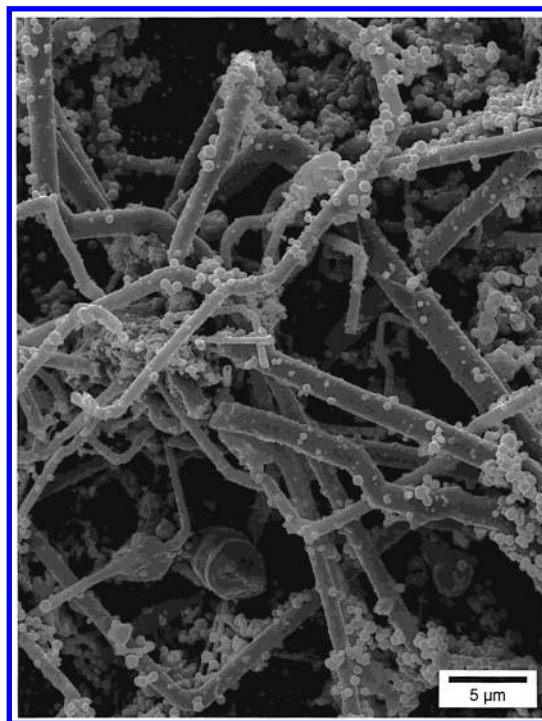


Figure 6. SEM of the tubular precipitate obtained with 5% $(\text{NH}_2\text{OH})\text{H}_2\text{SO}_4$.

spans from tens to several hundreds of nanometers (Figure 4c). Such a polydispersity is typical for the tubular vesicles of lipids.¹⁶ The SEM images reveal an abundance of conformations of the tubes, most of them being entangled. Microscopy also shows that the tubes always coexist with spherical particles or “vesicles” (Figures 6–8). The spheres and the tubules often interpenetrate and give complex hybrid forms.

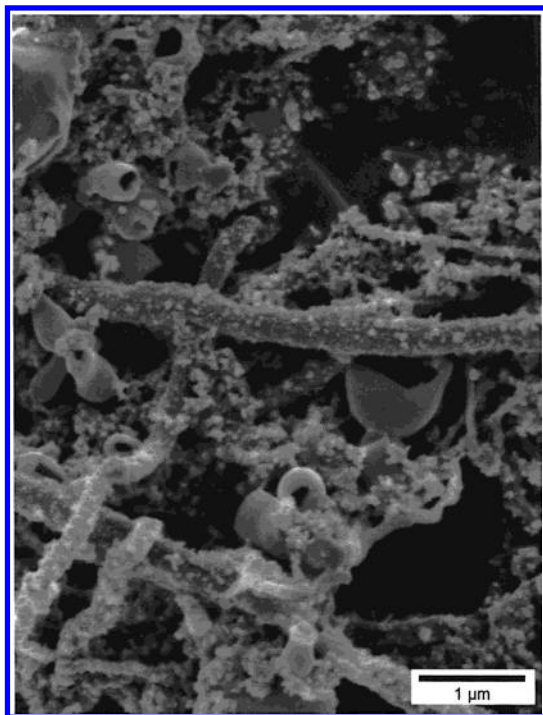


Figure 7. SEM of the tubular precipitate obtained with 10% KCl.

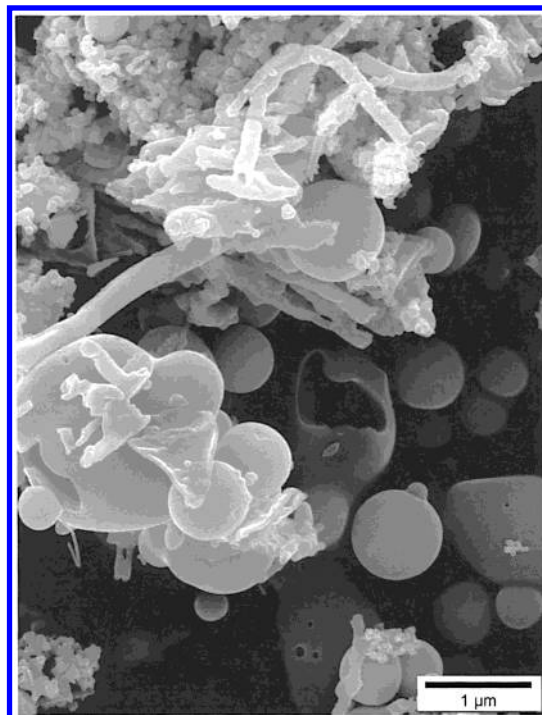


Figure 9. Tubules and broken hollow spheres in the precipitate obtained with 10% $(\text{NH}_2\text{OH})\text{H}_2\text{SO}_4$.

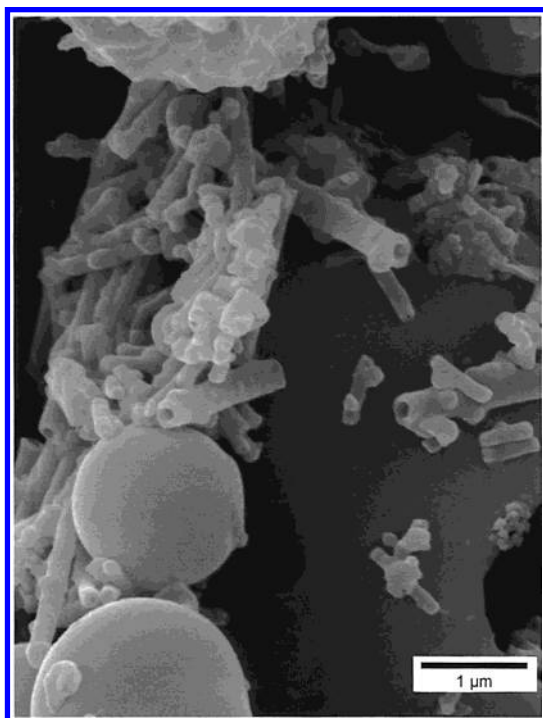


Figure 8. SEM of the tubular precipitate obtained with 10% NH_4SCN .

At higher electrolyte amounts (concentrated KCl or NH_4SCN , 20% vol of aqueous solution), the vesicle-like morphologies are destroyed, leaving place to the distorted lamellar or shapeless precipitate morphology appears (not shown). As a transient form, in the narrow range of conditions, sponge-like fractal structures are formed, containing hierarchically organized thin wall compartments (Figure 10).

The effects observed are electrolyte non-specific, i.e., the same types of structures are produced while the electrolyte amount in the reaction mixture increases (cf. Figures 6–8). Moreover, the electrolytes which are differently placed in the Hoffmeister series (strongly salting out $(\text{NH}_4)_2\text{SO}_4$, weakly

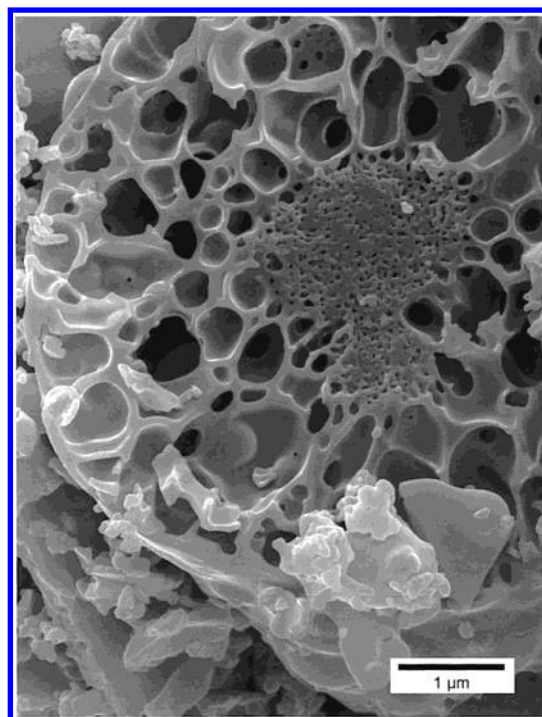


Figure 10. Fractal sponge-like solid obtained from the solid **I** in the presence of 20% NH_4SCN .

salting out KCl, or salting in NH_4SCN), give the same effect. This excludes the eventual influence of the formation of the electrolyte salt microcrystals in the course of precipitate formation. While the electrolyte amount increases, the morphology changes first from the shapeless matter mixed with microspheres to hollow spheres, then to the tubules, and finally to the large fractal assemblies and distorted lamellae. This sequence strongly resembles the behavior of the assemblies of amphiphilic molecules as a function of the packing parameter, while the system obeys the qualitative rules outlined by

Israelashvili et al. for the organic micelles.¹⁷ The decrease of the packing parameter upon the increase of the ionic strength is expected from the classical Debye Huckel theory.

The variations of the ionic force are known to influence the size and the relative stability of the liposomes and vesicles.^{18,19} However, the vesiculation onset is known to be favored by the nonzero spontaneous curvature of the layers.²⁰ The last might be generated if the chemical species or their combinations possess some asymmetry, as in the case of mixtures of single-tail surfactants having different chain length.²¹ In the systems considered here, the asymmetry and by consequence the non-zero curvature might be related to the structure of the oxosulfide oligomers. Indeed, almost all the known compounds containing the $\text{MoS}_2\text{O}_2^{4+}$ have the syn configuration of $\text{Mo}=\text{O}$ bonds (Scheme 1).²² Theoretical calculations also show that in the oxosulfide species the syn configuration is energetically favorable compared to the anti configuration.²³ In the syn configuration the slight bending of the MoSSMo planes exists along the $\text{S}-\text{S}$ axis. Being of the same sign in the neighboring dimeric $\text{Mo}-\text{Mo}$ moieties, constituting the oligomers, such bending may provide therefore the natural source of spontaneous curvature of condensed oxothiomolybdates. Indeed, it is well-known that the oxosulfide core $\text{MoS}_2\text{O}_2^{4+}$ easily forms the ring-shape clusters with all $\text{Mo}=\text{O}$ bonds directed outside the rings.^{24,25} The $\text{Mo}-\text{Mo}$ angles in such supramolecular wheels vary from 180° to 135° . The last structures are solved by X-ray structural analysis for the monocrystals of molecular compounds, but the same tendency will probably persist in the amorphous solids containing ill-defined oligomers. This may be an additional factor in the formation of vesicle-like morphologies in our systems. To verify whether the Mo oxosulfide oligomers have the tendency to form tubes and vesicles, the reactions of the individual $\text{MoO}_x\text{S}_{2-x}$ precursors will be studied soon.

The chemical nature of the oligomers is of obvious importance. From the general physical considerations it can be expected that the chain-like or branched geometry, flexibility, and above-mentioned spontaneous curvature are crucial for obtaining organized morphologies. However, independently on the exact chemical structure of the species, the main idea of this work is that carrying out a slow polymerization reaction in a mixed solvent in the presence of an electrolyte provides the possibility for the growing oligomers to self-organize, leading to complex patterns. Imperatively, some short-range attraction and long-range repulsion forces must be present in a system for any space self-organization to occur. In our case, the role of short-range attraction can be tentatively attributed to the interactions of the electrolyte ions with the ionic and polar $\text{Mo}=\text{O}$ moieties of the growing oligomers, whereas selective structuring of water and acetone around the differently charged areas of the oligomers should correspond to the long-range repulsion. Such a qualitative consideration provides a minimal basis to rationalize our findings. Note that there is no need for the presence of any organic surfactant template, or rather, growing oligomers are their own templates. Since the structures were observed not in the liquid phase but in the powder

precipitates, it was also important for our study that the polymerization continued in the assemblies of the oligomers and lead to rather rigid structures, which sustained centrifugation and drying and therefore could be observed by scanning electron microscopy. This point differentiates the objects reported here from the organic vesicles and micelles, which are stable only in solutions and therefore require cryomicroscopy for their observation.

The phenomenon observed might probably be extended to other inorganic systems. Moreover, since the molybdenum sulfides are very labile and difficult to study, we are now looking for some simpler objects and reactions showing similar self-organizing behavior. The common theoretical basis of the description of such systems should present a natural extension of the existing approaches. Indeed, though the theories describing the formation of micelles and vesicles have been developed having in mind the organic amphiphilic molecules, the physical equations derived and the general rules of behavior following from them are indifferent to the exact chemical nature of the self-organizing objects.

References and Notes

- (1) Iijima, S. *Nature* **1991**, 354, 56.
- (2) Saupe, G. B.; Waraksa, C. C.; Kim, H.-N.; Han, Y. J.; Kaschak, D. M.; Skinner, D. M.; Mallouk, T. E. *Chem. Mater.* **2000**, 12, 1556.
- (3) Adachi, M.; Harada, T.; Harada, M. *Langmuir* **2000**, 16, 2376.
- (4) Meng, Z.; Peng, Y.; Qian, Y. *Chem. Commun.* **2001**, 469.
- (5) Afanasiev, P.; Geantet, C.; Thomazeau, C.; Jouget, B. *Chem. Commun.* **2000**, 12, 1001.
- (6) Peng, Y.; Meng, Z.; Zhong, C.; Lu, J.; Yang, Z.; Qian, Y. *Mater. Chem. Phys.* **2002**, 73, 327.
- (7) Aberdam, D. J. *Synchrotron Radiat.* **1998**, 5, 1287.
- (8) Rehr, J. J.; Zabinsky, S. I.; Albers, R. C. *Phys. Rev. Lett.* **1992**, 69, 3397.
- (9) Bezverkhy, I.; Afanasiev, P.; Lacroix, M. *Inorg. Chem.* **2000**, 39, 5416.
- (10) Afanasiev, P.; Xia, G. F.; Berhault, G.; Jouguet, B.; Lacroix, M. *Chem. Mater.* **1999**, 11, 3216.
- (11) Afanasiev, P.; Bezverkhy, I. *Chem. Mater.* **2002**, 14, 2826.
- (12) Coucovanis, D. Koo, S. M. *Inorg. Chem.* **1989**, 29, 2.
- (13) Müller, A.; Sarkar, S.; Bhattacharyya, R. G.; Pohl, S.; Dartmann, M. *Angew. Chem., Int. Ed. Engl.* **1978**, 17, 535.
- (14) Mauge, F.; Lamotte, J.; Nesterenko, N. S.; Manoilova, O.; Tsygankenko, A. A. *Catal. Today* **2001**, 70, 271.
- (15) Hadjikyriacou, A. I.; Coucovanis, D. *Inorg. Chem.* **1989**, 28, 2169.
- (16) Chiruvolu, S.; Warriner, H. E.; Naranjo, E.; Idziak, S. H. J.; Radler, J. O.; Plano, R. J.; Zasadinski, J. A.; Safinya, C. R. *Science* **1994**, 266, 1222.
- (17) Israelachvili, J. L.; Mitchell, J. D.; Niham, W. B. *J. Chem. Soc., Faraday Trans.* **1976**, 272, 1525.
- (18) Robinson, B. H.; Bucak, S.; Fontana, A. *Langmuir* **2000**, 16, 8231.
- (19) Carrion, F. J.; de la Maza, A.; Parra, J. L. *J. Colloid Interface Sci.* **1994**, 164, 78.
- (20) Lasic, D. D.; Joannic, R.; Keller, B. C.; Frederik, P. M.; Auvray, L. *Adv. Colloid Interface Sci.* **2001**, 89–90, 337.
- (21) Yacilla, M. T.; Herrington, K. L.; Brasher, L. L.; Kaler, E. W.; Chiruvolu, S.; Zasadinski, J. A. *J. Phys. Chem.* **1996**, 100, 5874.
- (22) Shibahara, T. *Coord. Chem. Rev.* **1993**, 123, 73.
- (23) Duclusaud, H. Thesis, Lyon, 2001.
- (24) Dolbecq, A.; Cadot, E.; Sécheresse, F. *Chem. Commun.* **1998**, 2293.
- (25) Salignac, B.; Riedel, S.; Dolbecq, A.; Sécheresse, F.; Cadot, E. *J. Am. Chem. Soc.* **2000**, 122, 10381.